

POST-YIELD SHEAR FAILURE OF RC COLUMN AND ITS DUCTILITY SIMULATION

K. Maekawa

Department of Civil Engineering, The University of Tokyo, Tokyo, Japan

X. An

Tokyo Electric Power Services Co., Ltd., Tokyo, Japan

Abstract

In this paper, shear capacity and ductility of RC columns in the post-yield range of reinforcement are discussed for seismic resistant design. The shear failure of large scale RC column is computationally simulated for understanding the mechanism of shear collapse of bridge piers. FEM computational results on ductility are compared with the experiments and parametric study is conducted concerning factors that affect the deformability of RC columns.

Key words : Shear, ductility, RC column, FEM

1 Introduction

Through the investigation of RC columns for bridge piers that failed in the Hanshin-Awagi Earthquake, Okamura et al. (1995), it was found that there were two kinds of typical damages occurring for columns with different

dimensional features. For columns with smaller section and large span to depth ratio, greater deformation is supported to follow yielding of main reinforcement accompanying residual flexural crack opening. But no catastrophic collapse occurred in this kind of RC columns. The repair of RC columns damaged in flexural mode was not so difficult in practice. This is an important point in view of conservation of transportation capability. Another kind of damage is an unstable and brittle catastrophic shear failure. There are many RC piers with comparatively smaller shear span to depth ratio, larger scale of the sections, small main reinforcement ratio and much less web reinforcement. It seems that these RC columns with diagonal shear cracks lose the load carrying mechanism just after the shear failure and suddenly lose their function as bridge piers. This kind of collapse is very dangerous and should be avoided even in the case of strong earthquake beyond expectation.

In this paper, the shear collapse mechanism and ductility of RC column in the post-yield range of reinforcement are discussed, numerically simulated and understood in terms of the reduction of shear capacity associated with deformation. In order to simulate the unstable shear propagation of diagonal crack prior or after yield of main reinforcement, besides tension/shear stiffening models of RC, tension/shear softening models of concrete are also adopted in the FEM tool.

2 Mechanism of shear failure after yielding of main reinforcement

The shear capacity when yield of web reinforcement occurs can be formulated as sum of the shear force carried by concrete and that carried by web reinforcement. Then, we have,

$$V = V_c + V_s \quad (1)$$

where, V : total shear capacity of an RC member (yield capacity of web reinforcement), V_c : shear carrying capacity of concrete, V_s : shear carrying capacity of web steel based on yield.

If the shear capacity is larger than the shear force when yield starts, shear failure before yielding can be avoided. Here, we have,

$$V > P_y \quad (2)$$

where, P_y : shear force that brings about yielding of longitudinal reinforcement.

As the shear force carried by concrete may decrease after plasticity of main reinforcement, the post-yield shear capacity can be formulated as,

$$V = V_c^* + V_s \quad (3)$$

where, V_c^* : decreased shear carrying capacity of concrete.

The reduction of shear capacity related to deformation and crack propagation is indirectly taken into account by using reinforcement ratio in the code equations when we discuss pre-yield shear failure of RC beams. Similarly, the shear carrying capacity of concrete decreases after yield of main reinforcement and the total shear potential also decreases. It may result in smaller capacity than the applied shear force, and finally cause the lower ductility. The decrease in shear carrying capacity of concrete is an important factor that affects the deformational behavior of RC column.

Reference, Muguruma et al. (1985), discusses the shear force carried by concrete and web steel. In several RC columns, the relation of total shear force and averaged stress in web steel was recorded and the shear force carried by web and concrete was investigated as shown in Fig. 1.

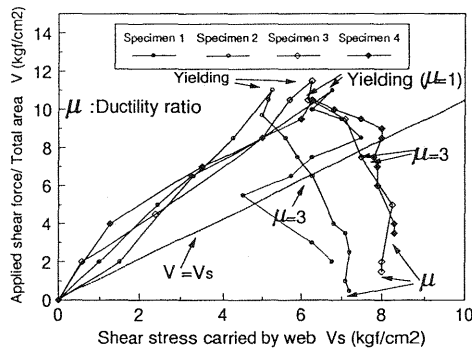


Fig. 1. Shear stress carried by web reinforcement from experiments, Muguruma et al. (1985)

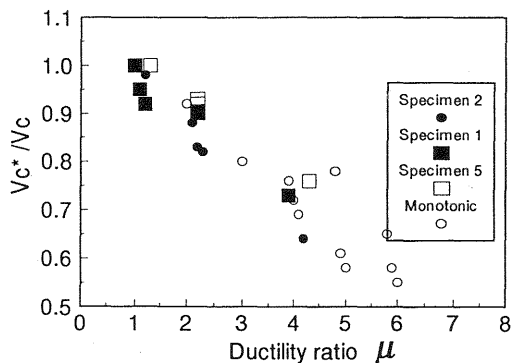


Fig. 2. Decrease in shear force carried by concrete after yielding of main reinforcement from experiments, Muguruma et al. (1985)

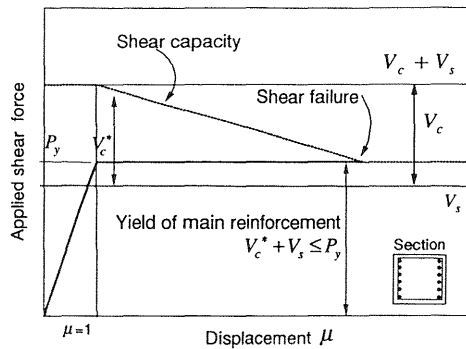


Fig. 3. Mechanism of shear failure after yielding of main reinforcement

It can be seen in Fig. 1 that the shear stress in web increases as the shear force is getting larger. And the shear force carried by concrete is kept almost constant before yield of main reinforcement. But after the yielding of main reinforcement ($\mu=1$, μ is defined as ductility index), the shear becomes smaller and smaller as the shear stress in web continues to be elevated. This phenomenon can be explained such that the shear force carried by concrete will decrease after plasticity of main reinforcement. This decrease is also shown in Fig. 2.

Based on the knowledge on the decaying shear capacity, post-yielding shear failure mechanism can be described as illustrated in Fig. 3. As the shear carrying mechanism is not fully understood, the FEM tool will be used for simulating the post-yield shear failure.

3 Nonlinear Constitutive models of reinforced concrete

In this research, FEM code WCOMD-SJ, Okamura et al. (1991), is used for ductility simulation of RC columns. Constitutive models adopted are proposed to simulate behaviors of RC members by finite element method for engineering proposes. The smeared crack model is used for cracked concrete with partially distributed fixed multi-directional cracks and all the stress-strain relationships are based on the spatial average stress and average strain of concrete defined in finite elements.

Owing to bond action between concrete and reinforcing bars, the concrete continues to support a part of tensile force even after cracking has taken place and been distributed in reinforced concrete area. In order to consider the influence of bond effects, the relation between the average stress and average strain of concrete is given as the macroscopic tension

model for cracked concrete. This tension model shows which is rooted in the stress transferred from steel bars to cracked concrete by bond effect, as shown in Fig. 4.

The cracked plain concrete shows strain-softening characteristics in tension comparing with the concrete confined by reinforcing bars. The stress-strain curve is decided with respect to the fracture energy and the crack band width, Bazant et al. (1983). In FEM computation, instead of the crack band width, reference length related to the element size is used to determine the mean stress-strain curve. The fracture energy is treated as a material property and needed to be kept constant regardless of the element size. Based on the fracture energy balance, the stress-strain curve defined in an element needs to be modified according to the reference length l_r (which is the square root of the element area as shown in Fig. 5). In the proposed model, An et al. (1997), the stiffening factor is adjusted with the element size by getting the constant fracture energy. Fig. 5 gives a series of tensile stress-strain curves used for the shear beam analysis.

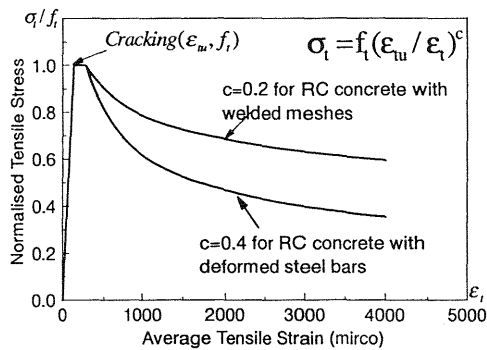


Fig. 4. Tension stiffening model for concrete in RC zone

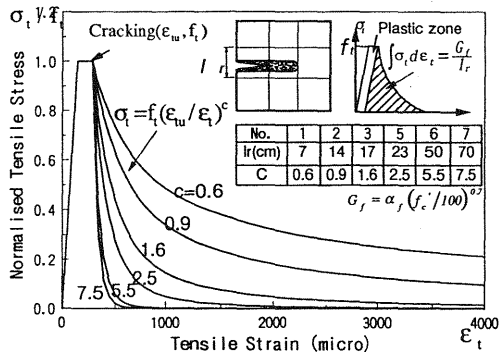


Fig. 5. Tension stress-strain softening curve in computation

In FEM computation, the whole RC member is to be divided into RC zone and PL zone. In each zone the suitable strain-stiffening or strain-softening model is to be adopted.

4 Failure mode and ductility Prediction of RC columns

It is well known that ductility of RC column is associated with shear carrying capacity. In ordinary cases, increase in web reinforcement exhibits higher ductility of RC columns and it is clearly shown by experiments, Ohta (1980) and Ishibashi et al. (1988). Here three experiments are reported with FEM simulations. The first and second cases are with joint element placed between footing and columns. The third one is a reinforced concrete column with side reinforcement.

The experimental details are shown in Table 1. The calculated shear capacities are listed in the table according to the JSCE code prediction and are larger than the shear force when yielding of main reinforcement occurs. Thus, the brittle shear failure before yielding is avoided. But the shear carrying capacity of each specimen is not so high as to exceed two times of shear force at yielding. According to the newly proposed criteria of JSCE, JSCE (1996), these specimens are expected to fail in shear mode after yielding of main reinforcement.

Table 1. Experiments of shear mode failure after yielding of longitudinal reinforcement

Series No.	1	1	1	2	2	3
Width B (cm)	80	80	80	40	40	40
Effective depth d (cm)	35	35	35	35	35	35
Shear span to depth ratio a/d	4.0	4.0	4.0	4.0	4.0	4.0
Axial stress (kgf/cm ²)	10	10	10	10	10	0
Main reinforcement ratio (%)	0.86	0.86	0.86	1.66	1.66	2.48
Web reinforcement ratio (%)	0.08	0.16	0.04	0.27	0.42	0.58
V_c (kgf/cm ²)	7.7	7.7	7.7	9.8	9.8	11.2
V_s (kgf/cm ²)	2.1	4.2	1.1	7.9	12.3	20.2
P_y (kgf/cm ²)	7.9	7.9	7.9	15.5	15.5	21.4
$(V_c+V_s) / P_y$	1.30	1.53	1.14	1.23	1.56	1.46
μ (By test)	3.9	4.2	3.0	5.0	7.0	5.9
μ (By FEM)	3.8	4.0	3.2	4.9	5.8	5.5
Failure mode	shear	shear	shear	shear	shear	shear

Note: No.1 from Ohta (1980), No.2 and No.3 from Ishibashi et al. (1988).

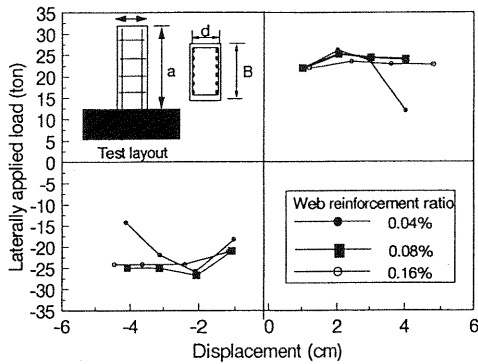
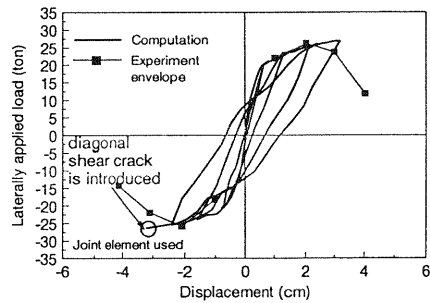
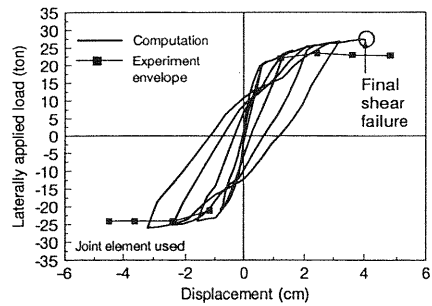
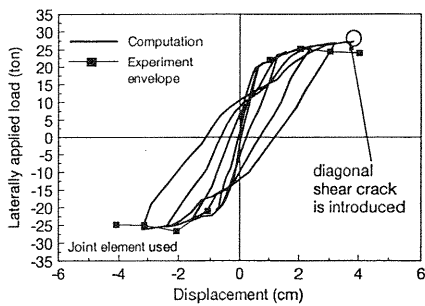


Fig. 6. Envelope of cyclic load-displacement relation of RC columns with different web reinforcement ratios, Ohta (1980)



(a) Web reinforcement ratio = 0.04%



(b) Web reinforcement ratio = 0.08% (c) Web reinforcement ratio = 0.16%
Fig. 7. Computed ductility and hysteretic responses

The FEM simulation on ductility associated with shear failure is verified by using the test data. Fig. 6 shows the target No. 1 of verification, Ohta (1980) and Fig. 10 of No.2, Ishibashi et al. (1988). The computed results are shown in Fig. 7 and Fig. 11. The computational loop will stop at the point that shear strain increases sharply and becomes larger than the critical

value (set as 1% in this research). The displacement at this point is taken as ultimate one, and the ductility at this point is used to compare with that at the point of maximum load in experimental loop, which continues after the peak of load and becomes smaller and smaller. It can be seen that FEM computed results have fair agreement with experimental ones. Both the experimental and computational results show that the increase in web reinforcement ratio in RC column yields higher ductility. In order to confirm the failure mode in computation, crack patterns of a specimen are shown in Fig. 8, with comparison of the observed shear cracks in experiment. The diagonal crack pattern is seen in experiment and analysis.

In order to confirm the behavior of joint element, the computed pull-out displacement for case 1 is compared with observed data in Fig. 9. The total displacement will increase about 30% because of this pull-out effect.

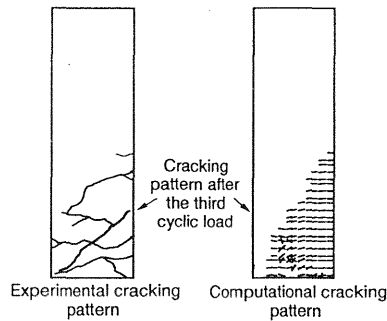
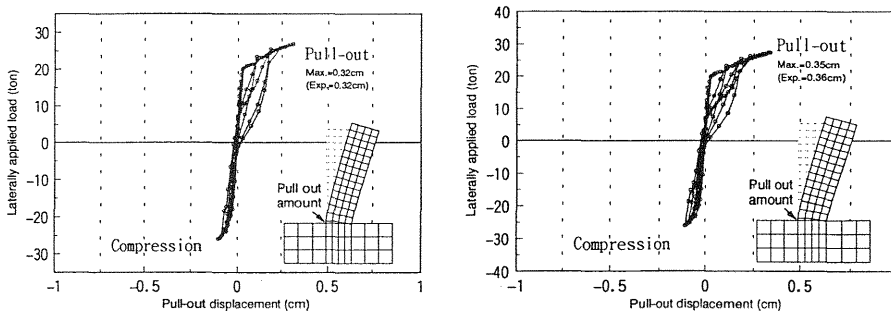


Fig. 8. Crack pattern comparison when shear failure occurs. (web reinforcement ratio=0.08%)



(a) Web reinforcement ratio =0.04% (b) Web reinforcement ratio =0.16%
Fig. 9. Pull-out displacement from computation

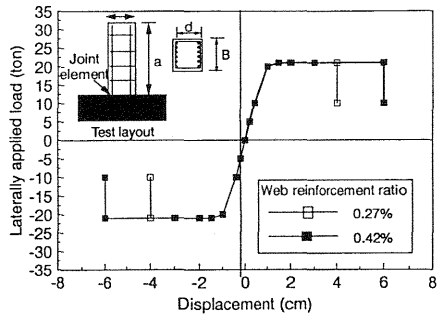
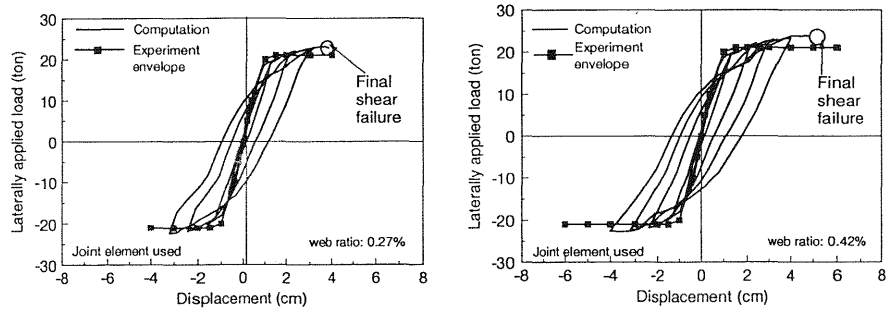


Fig. 10. Envelope of cyclic load-displacement relation of RC columns with different web reinforcement ratios



(a) Web reinforcement ratio=0.27% (b) Web reinforcement ratio=0.42%
Fig. 11. FEM simulation concerning the effect of web ratio on ductility

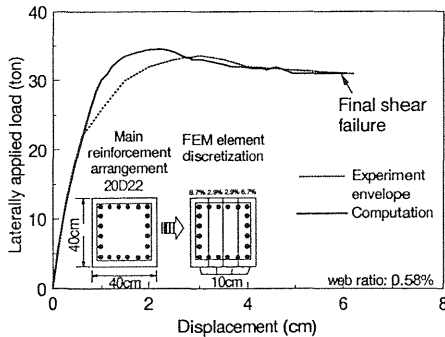


Fig. 12. FEM simulation for specimen with side reinforcement

The FEM simulation for RC column with side reinforcement under monotonic load is shown in Fig. 12. It is reported that side reinforcement atters shear carrying capacity prior to yielding of steel. The ductility of RC column with side reinforcement after yield of main reinforcement can also be simulated by FEM computation. All these results support that the shear

failure and ductility level of RC column after yielding of main reinforcement can be estimated by FEM analysis proposed in section 3.

Sectional sizes of all experiments are less than 1 meter. In this section, the shear failure before yielding of longitudinal reinforcement in $2\text{m} \times 2\text{m}$ scale RC column is simulated by FEM. In order to check the effect of web reinforcement on the failure mode and ductility, additional web reinforcement is placed to the referential case in the sensitivity analysis as listed in Table 2. The failure mode changes according to the different amount of web reinforcement ratio as calculated in Table 2. First, web reinforcement ratio is specified 0.15%. The total shear capacity is higher than shear load when yield occurs but the shear carrying capacity estimated by the JSCE code practice is much smaller than twice the shear load when yielding occurs. So, the column may fail in shear mode after yield of main longitudinal reinforcement resulting in less ductility.

If the web reinforcement is increased up to 0.2% by volume, the shear capacity is increased but is still lower than two times of the shear force at yielding force. Then, this case still brings shear failure, but higher ductility ratio can be expected. When the web reinforcement is increased to 0.35%, the shear capacity becomes higher than two times of the shear force at yielding point. In this case, brittle shear failure may be avoidable and the RC column may fail in flexure with high ductility.

Table 2. Failure mode prediction for large scale RC column

No.	1	2	3	4
Width B (cm)	200	200	200	200
Effective depth d (cm)	190	190	190	190
Shear span a/d	2.0	2.0	2.0	2.0
Main reinforcement ratio (%)	0.4	0.4	0.4	0.4
Web reinforcement ratio (%)	0.05	0.15	0.20	0.35
V_c (kgf/cm ²)	3.9	3.9	3.9	3.9
V_s (kgf/cm ²)	1.5	4.5	6.0	10.5
P_y (kgf/cm ²)	7.0	7.0	7.0	7.0
$(V_c+V_s) / P_y$	0.8	1.2	1.4	2.1
μ (By FEM)	<1.0	2.4	4.8	13.2

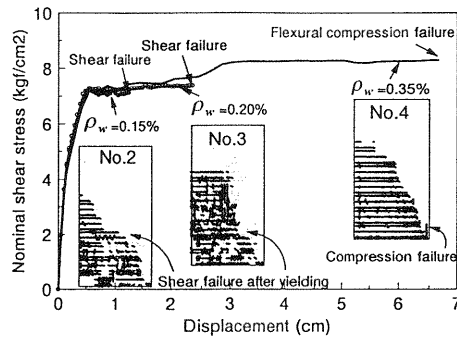


Fig. 13. Effect of web reinforcement ratio on ductility of large scale RC column in computation

All these cases are simulated in using nonlinear FEM as proposed in section 3. The analytical results under monotonic load are shown in Fig. 13. The failure mode is shown in the same figure with respect to crack patterns of the last computational step, that is the unstable failure point where progressive cracking is formed in iterative computation. From the crack patterns, it can be seen that the RC column No.2 and No.3 fail in shear mode after yield of main bars, but for No.4, the computation terminates in compression failure of concrete at extreme fiber close to the maximum moment section.

5 Parametric study on ductility of RC columns

In this section, FEM analysis is applied for parametric study on factors that influence the deformability, such as, main and web reinforcement ratios, axial force and shear span to depth ratio(a/d) of the column. Some experimental results will be employed for back check for versatility. The ranges of these parameters discussed are shown in Table 3.

Table 3. The range of parameters that affect ductility

Parameter	FEM	
Main reinf. ratio (%)	0.9-2.1	0.89--1.66
Web reinf. ratio(%)	0.08--0.36	0.08--0.23
Axial comp. stress(kgf/cm ²)	0--20	0-20
a/d	3-6	3-6

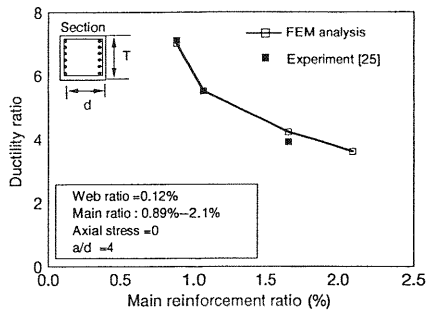


Fig. 14. Effect of main-bar ratio

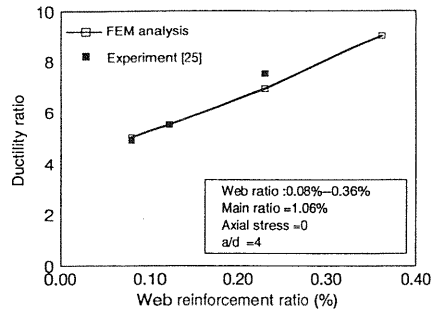


Fig. 15. Effect of web ratio

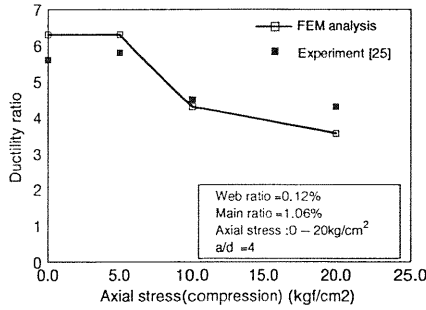


Fig. 16. Effect of axial stress

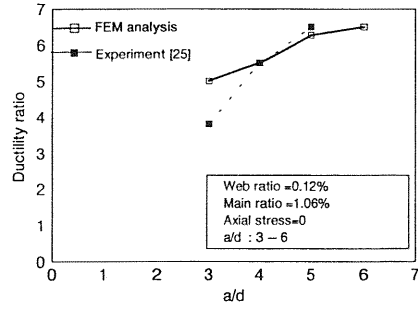


Fig. 17. Effect of a/d of column

All the computations are carried out under monotonic load. Details of computational targets and the results are shown in Fig. 14 to Fig. 17. For computing ductility factor, the definition of yield displacement is rather different among technical reports and vague for sections with side reinforcement. Within the scope of this study, the authors intentionally select specimens without side reinforcement. In this case, definition of yield displacement when bars start to yield is quite explicit, because main reinforcement gets plastic at the same time under flexure. We can consistently adopt the experimentally reported ductility from different investigators. From these results, some tendencies are clearly identified again as follows.

- As the main reinforcement ratio increases, the ductility decreases.
- The increase in web reinforcement ratio elevates the ductility of RC columns.
- The ductility tends to decrease when higher axial compressive force is applied.
- As the shear span to depth (a/d) ratio increases, the ductility also increases.

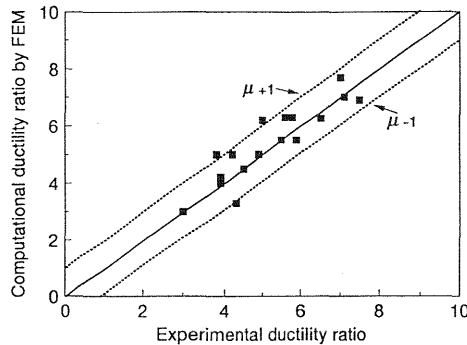


Fig. 18. Ductility ratio computed by FEM with the experimental results

Computed ductility ratios are summarized in Fig. 18, comparing with the experimental facts. It can be seen that the FEM simulation may give good prediction. The ductility associated with flexural action is out of discussion in this study, and further research on the buckling of bars and spalling of cover concrete will be needed.

6 Conclusion

The shear failure occurs even after yield of main reinforcement as the shear carrying capacity by concrete may decrease according to the plastic deformation of reinforcement. FEM code proposed was used for simulating the shear failure and ductility of RC columns. It was verified that the FEM computation has fair agreement with experimental facts and can deal with large scale sections. As it was found in experiment that main reinforcement, web reinforcement ratio, shear span to depth ratio and axial force may affect the ductility of RC columns, FEM was examined on how rationally the sensitivity of influencing factors would be predicted.

7 References

- An, X., Maekawa, K. and Okamura, H. (1997) Numerical simulation of size effect in shear strength of RC beams. **Journal of Materials, Concrete Structures and Pavements**, JSCE, No.564/V-35, 297-316.
- Bazant, Z.P. and Oh, B.H. (1983) Crack band theory for fracture of concrete, **Material and Structures**, (RILEM, Prais), Vol.16, 155-157.

Ishibashi, T. and Yoshino, S. (1988) Study on deformation capacity of reinforced concrete bridge piers under earthquake, **Journal of JSCE**, No.390/V-8, 67-67.

JSCE (1996) **Standard specification for seismic resistant design of concrete structure**, 1st ed, Tokyo.

Muguruma, H. and Watanabe, F. (1985) Strength evaluation of R/C column failing in shear, **Proc. of JCI**, Vol.7, No.2, 541-544.

Ohta, M. (1980) **A study on earthquake resistant design for reinforced concrete bridge piers of single-column type**, Report of civil research institute, No.153. Tokyo, Japan.

Okamura, H. and Maekawa, K., (1991) **Nonlinear Analysis and Constitutive Models of Reinforced Concrete**, Gihodo-Shuppan, Japan.

Okamura, H., Maekawa, K., Ozawa, K. and Ohuchi, M. (1995) Damage of concrete bridge piers, **Journal of JSCE**, Vol.80, No.4, 11-19.